chemical methods[1] in the degree of cationization. Typically, these wet methods produce a high intensity of substrate-cationized quasi-molecular and parent ions. These data support the idea of cationization in these systems as coordination of silver ions to the double bonds in unsaturated acids in the selvage during desorption; the lack of cationization in the saturated fatty acid systems would suggest that silver coordination does not occur at the acid head. Additionally clear differences are observed in relative intensities of quasi-molecular ions between wet oxidized syringe preparations from solution and LB preparations of monolayers. This points out the need to control orientation to understand chemical effects on ion production in SIMS. Because of the high intensities of characteristically even-numbered fragment ions, it is possible to distinguish unsaturation in the monolayer.

Additional research will focus on the influence of cations placed in the trough subphase as matrix assist agents, various substrates such as Au and Cu, surface tension during production, and the examination of Blodgett orientations in multilayers.

Acknowledgment. We thank Dr. R. E. Baier, M. Fornalik, and A. Meyer of Calspan Advanced Technology Corp. for advice and the use of the Langmuir-Blodgett equipment. Acknowledgement is made to the Donors of the Petroleum Research Fund, administered by the American Chemical Society, for partial support of this research. This investigation was also supported in part by a Research Development Fund Award from the State University of New York Research Foundation. Partial support by NSF Grant DMR 8412781 from the Polymers Program of the Division of Materials Research is also gratefully acknowledged.

Registry No. Lauric acid, 143-07-7; palmitic acid, 57-10-3; stearic acid, 57-11-4; oleic acid, 112-80-1; linolenic acid, 463-40-1; silver, 7440-22-4.

Chemical Ionization/Fast-Atom Bombardment Mass Spectrometry: Ion/Molecule Reactions†

Royal B. Freas,‡ Mark M. Ross, and Joseph E. Campana*

Contribution from the Naval Research Laboratory, Chemistry Division, Washington, D.C. 20375-5000. *Received October 30, 1984*

Abstract: A novel, high-pressure, fast-atom bombardment (FAB) ion source has been constructed in which ion/molecule reactions of sputtered ions and neutrals can be studied. A variety of ion/molecule reactions are reported on model systems that characterize the important features of this technique. The postdesorption reactions of sputtered species, ions and neutrals, increased the abundance of an $[M + H]^+$ species by almost 3 orders of magnitude. Enhancements in molecular parent ion abundances are shown to result from collisional stabilization, charge-exchange, chemical-ionization, and association reactions. Collisional stabilization of sputtered ions was affected by the different buffer gases, He, Ar, Xe, CO, CO_2, CH_4, and i-C_4H_{10}, and the abundances of molecular parent ions varied in direct proportion to the relative collisional stabilization efficiency of each buffer gas. Results of postdesorption ionization and collisional stabilization are discussed with regard to positive and negative ions of tetraesters and fatty acids.

Introduction

Fast-atom bombardment (FAB) mass spectrometry has proven to be a useful desorption technique for the characterization of intractable chemical species.[1] The FAB mass spectra of involatile middle molecules have yielded both molecular weight and structural information,[2] and many of the major fragmentations in the FAB mass spectra are reported to be similar to those observed by chemical ionization (CI) mass spectrometry.[3] In fast-atom bombardment mass spectrometry (FABMS), secondary ions and neutrals are sputtered from a solid surface, film, molecular overlayer, or a liquid matrix by a primary beam of energetic atoms. Similar emission processes also occur in other particle-induced emission techniques such as secondary ion mass spectrometry (SIMS). The secondary ions, desorbed in these methods, are analyzed by using conventional mass spectrometric techniques.

Several different processes in the particle bombardment process occur yielding various secondary particles. The events include negative and positive ion ejection and desorption of neutral species from the bombarded substrate.[4] The secondary ions and neutral species include molecular species and their fragments and clusters.[5]

The number of sputtered or desorbed neutral organic species should be considerably larger than the number of desorbed molecular ions. This assumption is based on ion and sputter yields from classical surface studies (metallic substrates) where typical sputter yields (atoms removed/incident particle) range[6] from 0.1 to 10 and positive ion yields (atomic ions/incident particle) range[7] from 1.0 to 1×10^{-4}. Our assumption can be supported and generalized further, based on the results of two studies. The first study showed that typical positive ion yields of organic molecules on a silver substrate (monolayer coverage) are on the order of 5×10^{-2} secondary ions per incident primary particle.[8] The second study demonstrated that ion yields for organic molecules sputtered from a silver surface and from a glycerol matrix are the same order of magnitude.[9] If the molecular neutral yields are significantly greater than the molecular ion yield, as we contend and all the above data indicate, then a simple method for the ionization of the abundant sputtered neutral species will yield increased

† This paper was presented in part at the 32nd Annual Conference on Mass Spectrometry and Allied Topics, San Antonio, Texas, May 1984.

‡ National Research Council Cooperative Research Associate.

* Author to whom correspondence should be addressed. Present address: Environmental Research Center, University of Nevada, Las Vegas, NV 89154.

(1) Barber, M.; Bordoli, R. S.; Elliott, G. J.; Sedgwick, R. D.; Tyler, A. N. *Anal. Chem.* **1982**, *54*, 645A-657A.
(2) Fenselau, C. *Anal. Chem.* **1982**, *54*, 105A-116A.
(3) Rinehart, K. L. *Science (Washington, D.C.)* **1982**, *218*, 254-260.
(4) Murray, P. T.; Rabalais, J. W. *J. Am. Chem. Soc.* **1981**, *103*, 1007-1013.
(5) Campana, J. E.; Ross, M. M.; Rose, S. L.; Wyatt, J. R.; Colton, R. J. "Ion Formation from Organic Solids"; Benninghoven, A., Ed.; Springer-Verlag: Berlin, 1983.
(6) Andersen, H. H.; Bay, H. L. "Sputtering by Particle Bombardment I."; Behrisch, R., Ed.; Springer-Verlag: Berlin, 1981, pp 145-218.
(7) Benninghoven, A. *Surf. Sci.* **1975**, *53*, 596-625.
(8) Benninghoven, A.; Sichtermann, W. *Int. J. Mass Spectrom. Ion Phys.* **1981**, *38*, 351-360.
(9) Benninghoven, A.; Junack, M.; Sichtermann, W., to be published. Junack, M. Doctorate Thesis, University of Munster, Munster, FRG, 1985.

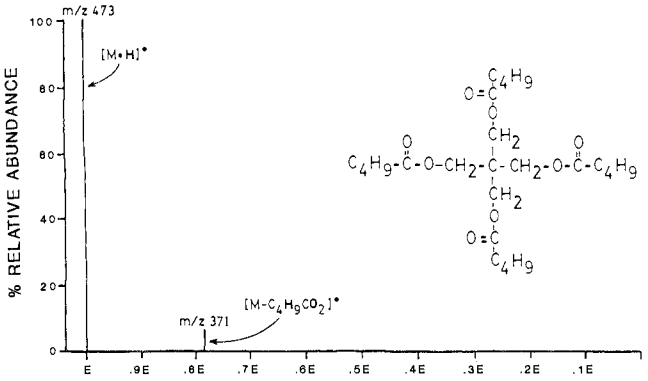

Figure 1. Mass-analyzed ion kinetic energy spectrum (unimolecular dissociation) of the protonated molecule of PETP.

abundances of molecular or fragment ions for analytical and fundamental studies. This postdesorption ionization process could result in increased detection limits of 2–3 orders of magnitude in the particle-induced emission techniques.

Early experiments on postdesorption ionization (or sputtered-neutral mass spectrometry) involved the electron ionization of species sputtered from metals and metal carbides.[10] Other investigators have used glow discharges,[11] plasmas,[12] and thermal ionization[13] to ionize sputtered inorganic neutrals. More recently, a multiphoton ionization technique of sputtered neutrals has been described for the characterization of materials.[14] Chemical ionization has been used in one laboratory to postionize laser-desorbed neutrals.[15]

An alternative approach to the method of postdesorption ionization of sputtered neutrals has been investigated in our laboratory; a high-pressure, fast-atom bombardment ion source has been constructed to study the chemistry and ion/molecule reactions of sputtered ions and neutrals.[16] Here, we report in detail several studies that have been performed to characterize this chemical ionization/fast-atom bombardment (CI/FAB) or postdesorption chemical ionization (PDCI) technique.

Experimental Section

The CI/FAB mass spectra were obtained on a VG Analytical ZAB-2F double-focusing mass spectrometer[17] (Manchester, U.K.), and a resolving power of 1000 was used for all studies. This spectrometer was also used to perform the mass-analyzed ion kinetic energy spectrometry (MIKES) measurements.[17] The spectrometer was fitted with an Ion Tech saddle-field gun (Teddington, U.K.), and xenon was used as the fast-atom beam. The fast-atom beam energy was 8 keV, and the density of the atom beam corresponded to a current density of 1–10 $\mu A/cm^2$ in the conventional FAB ion source. The current density was an order of magnitude lower in the CI/FAB ion source because of the small fast-atom entrance aperture (vide infra).

The CI/FAB source was constructed from conventional VG Analytical EI/CI and FAB ion source parts with some modifications. The modifications to the CI source block include apertures for the admittance of the fast-atom beam (0.050-in. diameter) and the FAB probe (ca. 0.50-in. diameter). An electrically insulating FAB probe extension was constructed from a resilient material (Vespel, E. I. du Pont de Nemours Co., Inc., Wilmington, DE) to mate tightly into the ion source and to replace the fragile ceramic tip. The conventional sample holders (1.5 mm × 5 mm stainless steel) were used in this insulating probe tip. Approximately 1 μL of neat sample was placed on the probe tip. Also, a smaller ion beam exit aperture (0.005 in. wide by 0.375 in. long) was constructed.

The distance that the fast-atom beam must traverse through the high-pressure source to impact the sample is about 1 cm. The mean-free path through 0.15 Torr of rare gas is about 10 cm, under the experimental conditions. There is no discernable difference in the secondary ion emission of atomic metal ions sputtered from a metal foil with or without a reactant gas in the CI/FAB ion source.

The abundances of the ions observed from the CI/FAB source are up to an order of magnitude less than the abundances from a conventional FAB source under the same conditions (no reactant gas or ionizing electrons). Experimental results indicate that this is due to the small ion beam exit aperture and not the small fast-atom beam entrance aperture. Under CI conditions, the source emission current was 1–5 mA and the electron energy was 100–200 eV.

The CI reactant gases and samples were obtained from commercial sources, and they were used without further purification. The pressures in the CI/FAB ion source were measured with a capacitance manometer pressure probe, similar to that recently reported,[17] and the pressures were either 0.15 or 0.2 Torr as noted. Because the pressure probe could not remain inserted in the ion source during high-voltage operation, it had to be replaced with the conventional solids probe during the experimental measurements. In other words, the pressure could never be measured during an experiment, only before and after. Therefore long-term drift

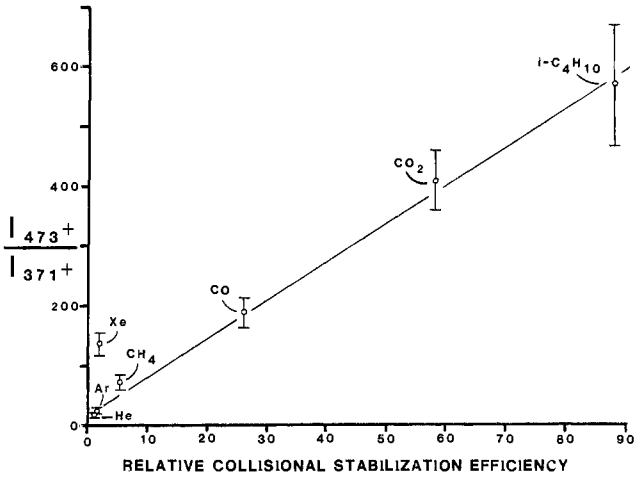

Figure 2. Ratio of the abundances of the protonated molecule ($[M + H]^+$, m/z 473) to the unimolecular dissociation product ion (loss of an acid moiety, m/z 371) vs. the relative collisional stabilization efficiencies (Appendix). The ionization was by fast-atom bombardment and the pressure of the buffer gases was 0.15 Torr. Error bars were determined by a propagational error analysis.

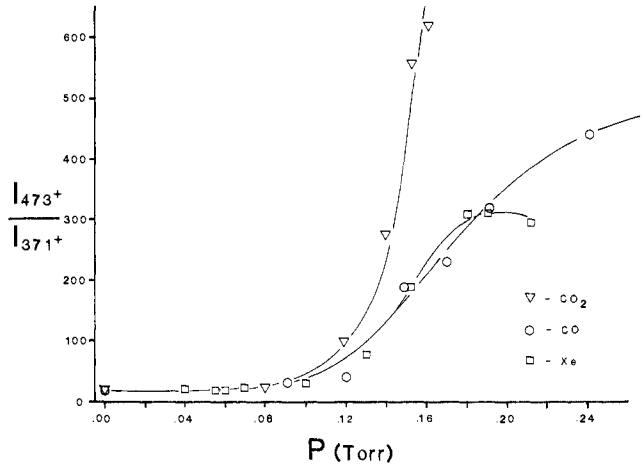

Figure 3. Ratio of the abundances of the protonated molecule ($[M + H]^+$, m/z 473) to the unimolecular dissociation product ion (m/z 371) vs. the pressure of three different bath gases, CO_2, CO, and Xe. The slopes of the linear portions of the lines are proportional to the collisional stabilization efficiencies of the gases.[21] The coincidence of the CO and the Xe curves implies similar collisional stabilization efficiencies, and this observation explains the disparity of the xenon data plotted in Figure 2 (see text for explanation).

(10) Honig, R.; *J. Appl. Phys.* **1958**, *29*, 549–555. Honig, R. "Advances in Mass Spectrometry, Vol. 2"; Elliott, R. M., Ed.; Macmillan: New York, 1963, pp 25–37.
(11) Coburn, J. W.; Tagluer, E.; Kay, E. *J. Appl. Phys.* **1974**, *45*, 1779–1786.
(12) Ishitani, T.; Sakudo, N.; Tamura, H.; Kanomata, I. *Phys. Lett.* **1978**, *67A*, 375–378. Oechsner, H.; Stumpe, E. *Appl. Phys.* **1977**, *14*, 43–47.
(13) Blaise, G.; Castaing, R. *Acad. Sci. Paris (Ser. B)* **1977**, *284*, 449–452. Hennequin, J. F.; Couchouron, M. *Rev. Phys. Appl.* **1979**, *14*, 993–1006.
(14) Winograd, N.; Baxter, J. P.; Kimock, F. M. *Chem. Phys. Lett.* **1982**, *88*, 581–584.
(15) Cotter, R. *Anal. Chem.* **1980**, *52*, 1767–1770.
(16) Campana, J. E.; Freas, R. B.; *J. Chem. Soc., Chem. Commun.* **1984**, 1414–1415.
(17) Morgan, R. P.; Beynon, J. H.; Bateman, R. H.; Green, B. N. *Int. J. Mass Spectrom. Ion Phys.* **1978**, *28*, 171–191.
(18) Guilhaus, M.; Gregor, I. K. *Org. Mass Spectrom.* **1985**, *20*, 312–313.

and short-term fluctuations were not observed, but they could bear on the quality of the pressure data presented in Figures 2 and 3. The pressure-dependent data given in Figure 2 are based on several experiments on different days, whereas the data given in Figure 3 are the averages of triplicate data obtained on 1 day. The agreement between Figures 2 and 3 is good considering a 5–10% estimated pressure measurement error, and the fact that the curves given in Figure 3 were fit by hand.

The ion abundance data reported for the ion/molecule reactions are free from contributions arising from sample vaporization and/or desorption chemical ionization. In the absence of the fast-atom beam, the sample within the chemical ionization plasma did not give significant abundances of ions; that is, they were 3–4 orders of magnitude less than the values we report here. However, these other processes could be significant at elevated ion source temperatures where sample volatilization and subsequent chemical ionization occurs. For this reason, care was taken to keep the ion source at ambient temperature. The electron filament was turned on only intermittently to take the appropriate measurements and to avoid ion source heating. Also, after the CI/FAB ion source was operated for several hours, some desorption chemical ionization was observed from contaminants (sputter products) deposited on the large internal surface area of the ion source. The CI/FAB ion source was cleaned frequently during these experiments to avoid contributions from desorption chemical ionization.

The mass spectra reported here were obtained by a data system. Any multiplication factors shown in the mass spectra apply to the entire spectrum except for those figures containing insets. Therefore, the spectra can be compared directly.

Results and Discussion

The postdesorption reactions of sputtered species can be accomplished by various ion/molecule reactions: chemical ionization, charge-exchange, and collisional stabilization. Reactant ions are formed within the CI/FAB ion source in a conventional manner, through the electron ionization of a reactant gas. The reactant species can be (a) ions resulting from secondary reactions of the reactant gas (chemical ionization),[19] (b) primary ions from the electron ionization of the reactant gas (charge exchange),[20] or (c) the neutral reactant gas (collisional stabilization).[21] These species then react with the sputtered sample species.

Collisional Stabilization. Collisional stabilization of sputtered ions was affected by different buffer gases: He, Ar, Xe, CO_2, CO, CH_4, and i-C_4H_{10}. The unimolecular dissociation of the protonated molecule of pentaerythritol tetrapentanoate (PETP) was observed to decrease in proportion to the relative collisional stabilization efficiency of the buffer gas. A mass-analyzed ion kinetic energy (MIKE) spectrum of the protonated PETP molecule is shown in Figure 1. The total unimolecular fragment ion abundance can be viewed as a relative measure of the internal energy of the molecular ion that leaves the ion source. The molecular ion was produced by fast-atom bombardment of the neat liquid sample, with no buffer gas in the ion source, and the MIKES spectrum was measured. Alternately, each of the several bath gases were introduced at a pressure of 0.15 Torr and MIKES spectra were recorded. Figure 2 depicts the ratio of the abundance of the $[M + H]^+$ species to the abundance of the sole unimolecular dissociation product at m/z 371 (loss of the acid moiety from the protonated molecule of PETP) vs. the relative collisional stabilization efficiency of each bath gas. (See Appendix for a discussion of the source of the relative collisional stabilization efficiencies used in this investigation.) As seen in Figure 2, the plot provides a good correlation between the relative ion abundance enhancements and the collisional stabilization efficiencies of the several different gases. An anomaly appears for the case of xenon. Because the energetic fast-atom beam also is xenon, collisional ionization of the xenon bath gas may be facile. The resulting xenon ions could then act as a charge-exchange reactant with the sputtered species such that collisional stabilization reactions no longer predominate. To test this hypothesis, the ion source electron filament was used to ionize the xenon bath gas, and the resulting ion abundance ratio was found to give nearly the same values as with the electron filament off. This result suggests that collisional ionization processes involving xenon collision partners and subsequent charge-exchange reactions may be responsible for the anomalous xenon data in Figure 2. (However, we show later that this interpretation is not necessarily correct.)

Table I. Relative Abundances[a] of $|PETP + H|^+$ under Different Ionization Conditions

gas	pressure = 0.15 Torr, ionizing filament off	pressure = 0.15 Torr, ionizing filament on
He	0.7	0.4
Ar	0.3	0.2
Xe	1	1
CO_2	3	33 (80)[b]
CH_4	5	90
i-C_4H_{10}	110	520 (850)[b]

[a] The ion abundances were averaged from several repetitive experiments, and they are relative to the abundance of the protonated molecule produced by fast-atom bombardment without gas in the CI/FAB source. The ion current measured for the protonated molecule under this condition was 1.5 pA. [b] The reactant gas pressure in this experiment was 0.2 Torr.

Figure 3 illustrates the change in the ratio of the abundance of the $[M + H]^+$ species to the abundance of the sole unimolecular dissociation product ion (loss of the acid moiety at m/z 371) of PETP vs. the pressure of CO_2, CO, and Xe bath gases. This figure shows that the ion abundance ratio is a function of unimolecular and collision-induced dissociation and the collisional stabilization efficiency of the buffer gas. As the pressure of the buffer gas increases beyond 0.1 Torr, the number of collisions occurring becomes large enough to stabilize effectively the $[M + H]^{+*}$ species produced by the bombardment of fast xenon atoms on a neat sample of PETP. Between 0.1 and 0.2 Torr, the slopes of the curves appear linear, and this linear portion is proportional to the collisional stabilization efficiency of the bath gases.[22] The change in the ion abundance ratio at higher pressures (>0.2 Torr) is due to scattering and collisional-induced dissociation of the ions accelerated out of the ion source, a result of the inefficient source-housing and first field-free region pumping of the buffer gas.

With regard to the anomaly in the xenon data in Figure 2 (vide supra), it should be noted that the slope of the curve for xenon in Figure 3 (0.1–0.2-Torr region) is almost coincident with the curve observed for CO. This suggests that the relative collisional stabilization efficiencies of xenon and CO are similar for the deactivation of excited PETP ions. If the collisional stabilization efficiency value used for CO in Figure 2 is used also for xenon, then the xenon data fall on the curve depicted in Figure 2. This explanation appears more reasonable than the charge-exchange explanation that we postulated above. (As explained in the Appendix, the collisional stabilization efficiencies were calculated from literature data.)

The results on collisional stabilization are interpreted to mean that the secondary molecular ions are ejected with excess internal energy, and many of the secondary ions can be collisionally stabilized in the high-pressure ion source before unimolecular dissociations can occur. This collisional stabilization can lead to the large relative molecular ion enhancements such as those that we have observed (Figures 2 and 3).

Postdesorption Ionization. The postdesorption reactions (ionization and collisional stabilization) of sputtered species have been observed to increase the abundance of the $[M + H]^+$ species of PETP by almost three orders of magnitude. Table I presents the changes in the abundance of the $[M + H]^+$ species with respect

(19) Field, F. H. *Acc. Chem. Res.* **1968**, *1*, 42–49.
(20) Einolf, N.; Munson, B. *Int. J. Mass Spectrom. Ion Phys.* **1972**, *9*, 141–160.
(21) Harrison, A. "Interactions Between Ions and Molecules"; Ausloos, P., Ed.; Plenum Press: New York, 1975; pp 263–278.
(22) For the reactions $473^{+*} + M \rightarrow 473^+$ with the collisional stabilization rate constant k_s, and $473^{+*} \rightarrow 371^+ + 102$ with the unimolecular dissociation rate constant k_d, the ratio $[473^+]/[371^+]$ can be expressed as $k_s[M]/k_d$ (generalized from ref 21, p 270). Analogous to the discussion in the Appendix, the latter term is proportional to the collisional stabilization efficiency of bath gas M.

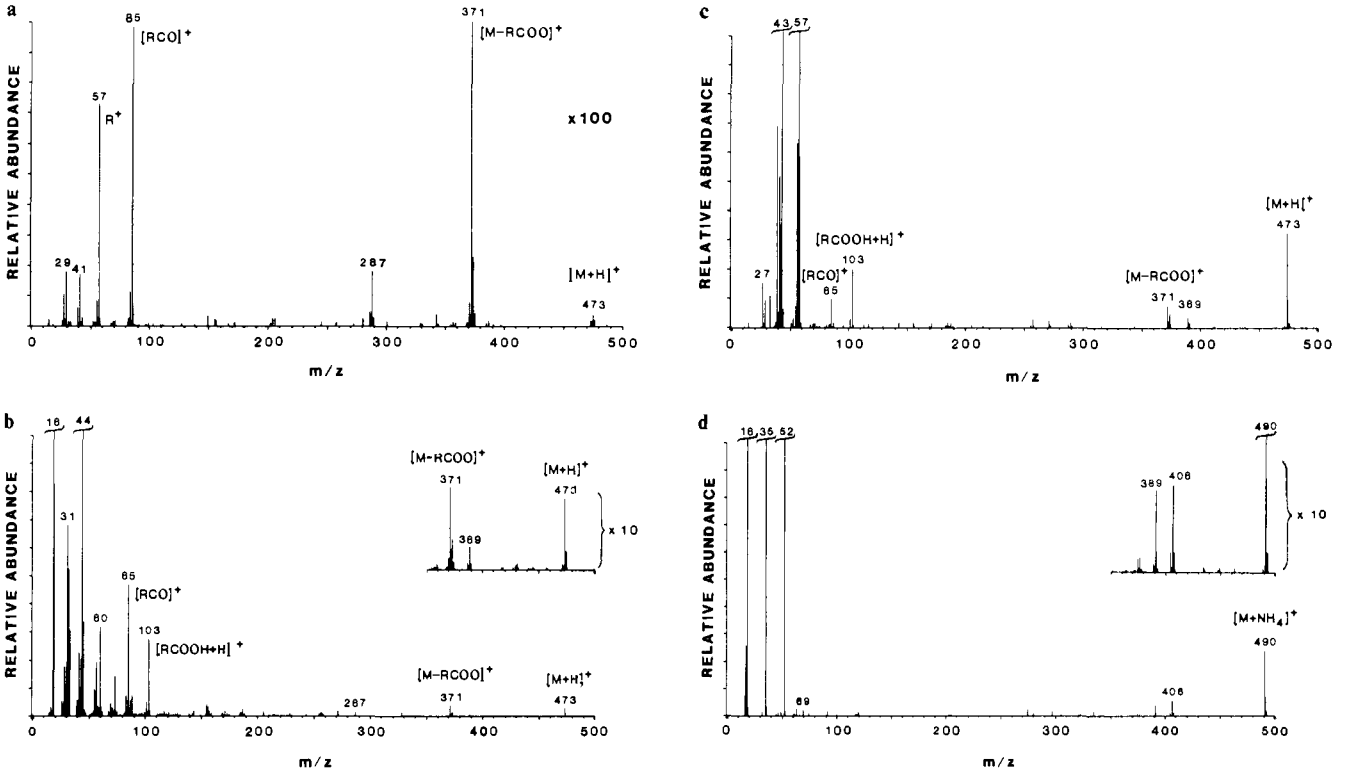

Figure 4. (a) Fast-atom bombardment mass spectrum of neat PETP obtained in the CI/FAB ion source with no reactant gas or ionizing electrons. The protonated molecule $[(M + H]^+$, m/z 473) is less than 5% of the base peak, $[C_4H_9CO]^+$. The protonated molecule is less than 0.5% of the base peak in the fast-atom bombardment mass spectra obtained in the conventional FAB ion source.[16] (b) CO_2 chemical ionization/fast-atom bombardment mass spectrum of neat PETP. The molecular ion ($[M + H]^+$, m/z 473) is almost 100 times more abundant than in the FAB spectrum shown in Figure 4a. The CO_2 pressure was 0.2 Torr. Major fragment ions are observed due to a loss of an acid moiety from the protonated molecule (m/z 371), a cyclic rearrangement yielding loss of the protonated pentanoic acid moiety at m/z 103 via a five-member cyclic transition structure and the acylium ion $[C_4H_9CO]^+$ at m/z 85. The protonated triester $[M' + H]^+$ impurity is observed at m/z 389. (c) Isobutane chemical ionization/fast-atom bombardment mass spectrum of PETP. The isobutane pressure was 0.2 Torr. The molecular ion ($[M + H]^+$, m/z 473) is almost 1000 times more abundant than in the FAB spectrum shown in Figure 4a. The $[M + H]^+$ species is more abundant than any of the fragment ions of PETP. (d) Ammonia chemical ionization/fast-atom bombardment mass spectrum of neat PETP. The molecular adduct ion $[M + NH_4]^+$ is almost 1000 times more abundant than the $[M + H]^+$ species in the FAB spectrum shown in (a). The ammonia pressure was 0.2 Torr. High-mass fragment ions are observed analogous to those seen in the CO_2 and the isobutane CI/FAB spectra of PETP.

to several different bath/reactant gases under different ionization conditions. With buffer gas present in the ion source, the absolute abundance of the protonated molecule is enhanced primarily by collisional stabilization; some charge exchange and chemical ionization can occur due to collisional ionization of the buffer gas by the fast xenon atom beam. When the ionizing filament is then turned on, the abundance of the molecular ion is increased by charge-exchange reactions and chemical ionization, which we assume dominate the molecular ion enhancement over collisional deactivation. Although carbon dioxide appears to be a relatively efficient collisional stabilization gas (better than methane) in Figures 2 and 3, the abundance of the protonated molecule of PETP is enhanced dramatically by proton-transfer reactions in the methane and isobutane systems. The ion abundances that are less than or equal to one (He, Ar, Xe) in Table I are a result of scattering and collision-induced dissociation of the molecular ion species in the first-field free region as discussed in the previous section. These effects are due to inefficient pumping of the rare gases, which leads to loss of the $[M + H]^+$ species.

Charge-Exchange Reactions. The ratio of the $[M + H]^+$ ion abundance of PETP to the unimolecular dissociation product ion abundance (m/z 371) generally decreases with increasing ionization potential of the gas used to generate the charge-exchange reactant ions. Table II shows this ion abundance ratio for different reactant gases at a pressure of 0.15 Torr. Other processes occurring within the CI plasma include collisional stabilization, proton transfer, charge exchange, association, and condensation reactions. These multiple effects are superimposed on the data shown in Table II, making interpretation difficult. The effect of charge exchange can be seen best by comparing the data for He, Ar, and Xe, whose collisional stabilization efficiencies are about

Table II. Charge-Exchange-Induced Fragmentation of Protonated PETP[a]

gas	IP, eV[b]	$I_{473}+/I_{371}+$
He	24.6	24
Ar	15.7	59
CO_2	13.7	109
CH_4	12.6	111
Xe	12.1	90
i-C_4H_{10}	10.7	300

[a] The ionizing filament and the fast-atom beam were on during the measurement of these data. The pressure of the gas was 0.15 Torr. [b] Rosenstock, H. M.; Draxl, K.; Steiner, B. W.; Herron, J. T. *J. Phys. Chem. Ref. Data, Suppl. 6*, **1977**.

unity (or in other words ineffective), and for which there is no contribution for proton transfer reactions. Generally, the ion abundance ratio increases as the ionization potential of the rare gas decreases. We postulate that the increase in the $[M + H]^+$ species is due to a gas-phase reaction sequence that involves charge exchange to low-mass neutral molecular fragments whose internal energies will be dependent on the nature of the charge-exchange species. The resultant (excited) fragment ions, which are not collisionally deactivated effectively in collisions with rare gas species, react by proton transfer to the sputtered molecular neutrals,[23] where they may also impart their excess energy. This, in part, explains why there is some correspondence between ionization potential and the ion abundance ratio.

(23) The reactions of internally excited H_3^+ with various species have been reported. See: Bowers, M. T.; Chesnavich, W. J.; Huntress, Jr., W. T. *Int. J. Mass Spectrom. Ion Phys.* **1973**, *12*, 357–382.

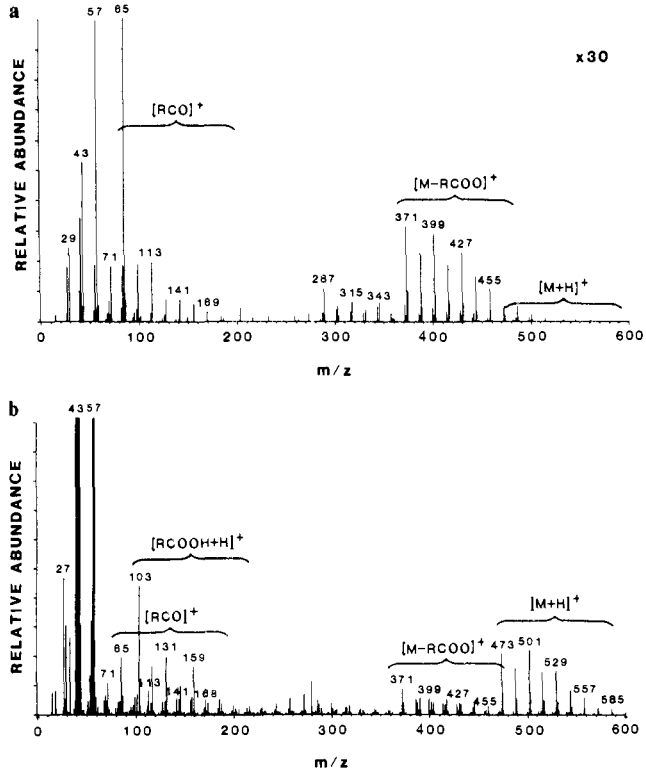

Figure 5. (a) Fast-atom bombardment mass spectrum of a homologous/isomeric mixture of neat pentaerythritol tetraalkanoates. The acid loss fragments of the high-mass homologues are observed in the molecular ion region of the low-mass homologues. The molecular ions are not observed in the spectrum. (b) Isobutane CI/FAB mass spectrum of the neat pentaerythritol tetraalkanoate mixture showing almost a 1000-fold increase in the protonated molecule abundances.

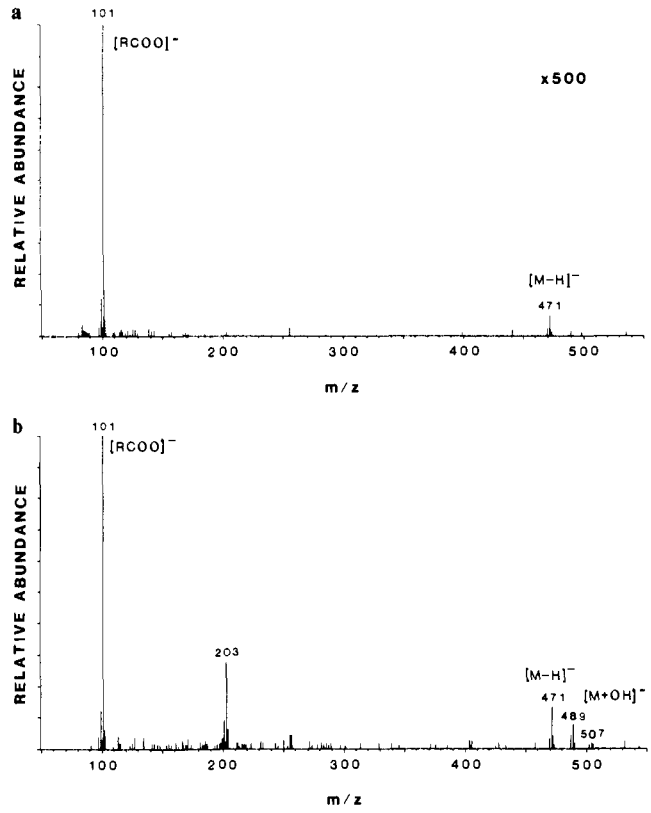

Figure 6. (a) Negative ion fast-atom bombardment mass spectrum of neat PETP. (b) H_2/N_2O [OH^-] negative ion chemical ionization/fast-atom bombardment mass spectra of neat PETP. The deprotonated molecule $[M - H]^-$ (m/z 471) is 1000 times more abundant than in the negative ion FAB spectrum shown in (a). The H_2/N_2O pressure was 0.2 Torr.

Positive Ion Chemical Ionization. The ion abundances of the $[M + H]^+$ species of PETP and its fragment ions change in a mass spectrum with the addition of reactant ions to the ion source. Enhancement of the protonated molecule occurs, and the relative abundances of the fragment ions of PETP diminish. Figure 4 displays mass spectra of PETP under four different ionizing conditions. Figure 4a presents a fast-atom bombardment mass spectrum of neat PETP without gas in the CI/FAB ion source. The protonated molecule (m/z 473) is less than 5% of the base peak ($[C_4H_9CO]^+$, m/z 85). A mass spectrum of PETP obtained in the conventional FAB source (not shown; see ref 16) shows a protonated molecule that is less than 0.5% of the base peak ($[C_4H_9]^+$, m/z 57). These differences are due to the closed volume and small primary beam entrance aperture of the CI/FAB ion source, which affect increased molecular ion abundance and decreased fragmentation through "self" chemical ionization and decreased radiation damage (vide infra), respectively.

Figure 4b shows a CI/FAB mass spectrum that was obtained with carbon dioxide present (0.20 Torr) and the ionizing filament on. The protonated molecule is almost 100 times more abundant than in the FAB spectrum shown in Figure 4a. In addition, the abundance of the fragment ion at m/z 371 is comparable to the abundance of the protonated molecule.

Figure 4c presents the isobutane CI/FAB mass spectrum of the PETP obtained at an isobutane pressure of 0.20 Torr. The resulting enhancement of the protonated molecule is almost 1000 times more abundant than in the FAB spectrum (Figure 4a). The protonated molecule now is clearly the most abundant ion above m/z 100.

The use of ammonia as a reagent gas results in the formation of an abundant $[M + NH_4]^+$ species as shown in Figure 4d. In this example with an ammonia pressure of 0.2 Torr, an $[M + NH_4]^+$ abundance almost 1000 times greater than the $[M + H]^+$ abundance obtained by FAB ionization (Figure 4a) was observed. The total fragmentation is negligible compared to the other spectra shown in Figure 4; the only significant molecular fragments observed are due to the loss of a C_4H_9COO moiety (m/z 389) from the molecular adduct ion. The m/z 406 species is the $[M' + NH_4]^+$ adduct of the triester impurity. The ammonia reagent gas cluster series $[(NH_3)_n{\cdot}NH_4]^+$ for n = 0, 1, 2, and 3 is also observed. In a complementary experiment, PETP and ammonium chloride were admixed and analyzed by conventional FABMS. The $[M + NH_4]^+$ species was not observed from this admixture as reported for different types of compounds by others.[24] This suggests that these gas-phase reactions are more facile than those within a matrix.

The tremendous enhancements in molecular ion yields realized by the CI/FAB technique have permitted the determination of the composition of a commercial mixture of pentaerythritol tetraalkanoates[25] where each of the four acid moieties of the tetraester molecule can have carbon chains of C_4 to at least C_{10}. The FAB spectrum of this mixture is shown in Figure 5a. It is dominated by those fragments resulting from the loss of an acid group. Many of these fragment ions originating from the high-mass homologues are observed in the molecular ion region of the low-mass homologues, hence making a detailed determination of the isomers difficult. The isobutane CI/FAB spectrum of this mixture is shown in Figure 5b, where more than a 1000-fold enhancement is observed in the protonated molecular ion region. These abundant molecular species allow determination of the isomeric composition of the mixture at each isobar by use of tandem mass spectrometry techniques.[25]

Negative Ion Chemical Ionization. Figure 6 displays the negative ion mass spectra of PETP under conventional FAB and CI/FAB conditions. The FAB negative ion spectrum of PETP is shown in Figure 6a. The major ions that are observed are the $[M - H]^-$ (m/z 471) species and the carboxylate negative ion of the C_5 acid

(24) Dell, A.; Oates, J. E.; Morris, H. R.; Egge, H. *Int. J. Mass Spectrom. Ion Phys.* **1983**, *46*, 415–418.
(25) Campana, J. E.; Freas, R. B. *ASLE Trans.*, in press.

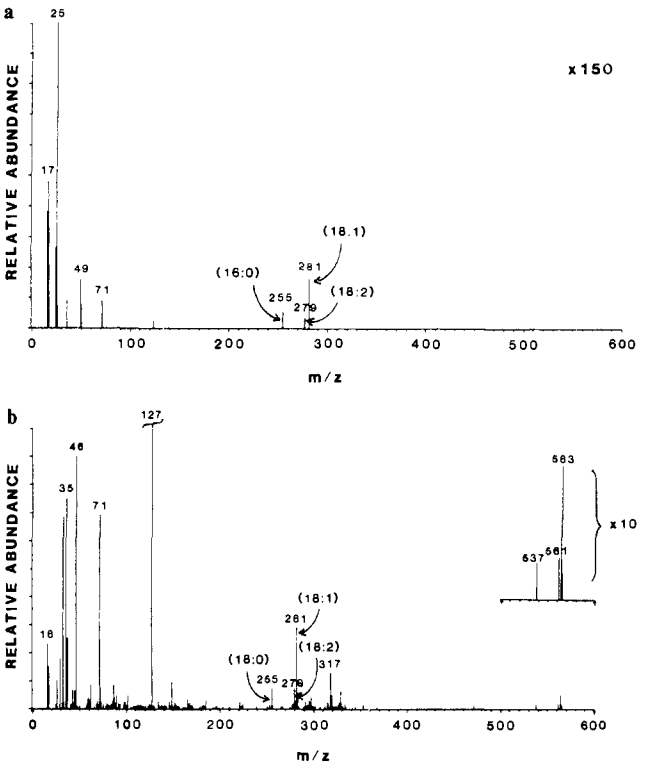

Figure 7. (a) Negative ion fast-atom bombardment mass spectrum of neat olive oil. (b) H_2/N_2O [OH^-] negative ion chemical ionization/fast-atom bombardment mass spectrum of neat olive oil. The carboxylate ions are 1000 times more abundant than in the spectrum shown in (a). The H_2/N_2O pressure was 0.2 Torr.

moiety $[(C_4H_9CO_2]^-$, m/z 101). Figure 6b shows the CI/FAB mass spectrum that was obtained with a mixture of H_2/N_2O (1:1) as the reagent gas mixture with the ionizing filament on. This gas mixture yields the OH^- reagent species, which can deprotonate some molecules.[26] The OH^- CI/FAB mass spectrum of PETP yields a 1000-fold enhancement of the $[M - H]^-$ abundance relative to the spectrum shown in Figure 6a. The $[M + OH]^-$ adduct species and an ion at m/z 203 are observed also in the OH^- CI/FAB mass spectrum of PETP, which are not present in the FAB mass spectrum. This latter ion corresponds to the negative ion dimer of the fatty acid moiety $[(RCOOH)_2 - H]^-$ from the PETP molecule, which may be written equivalently as the proton-bound dimer of the carboxylate anions ($RCOO^-\cdots H^+\cdots{}^-OOCR$). Ionic clusters such as these have been observed also in the CI/FAB spectra of pure fatty acids and esters.[27]

The negative ion CI/FAB method has been used to determine the fatty acid composition of various lipids; an example obtained in our laboratory is with a vegetable oil. The traditional method for the analysis of fatty acids from lipids involves hydrolysis of the lipid to give the free acid followed by esterification of the fatty acids to yield the volatile methyl esters for gas chromatographic analysis. It has been shown in one GC/MS study that the use of an OH^- CI reagent ion yields abundant carboxylate negative ions ($[RCOO]^-$) from the fatty acids.[28] In addition, it has been demonstrated that underivatized fatty acids[29] also yield abundant carboxylate anions in negative ion FAB.

We demonstrate the OH^- CI/FAB method for the analysis of fatty acids from triglycerides in olive oil. The FAB spectrum of pure olive oil is shown in Figure 7a. The most abundant ions observed are those that correspond to the carboxylate negative ions of the fatty acid moieties from the triglyceride molecules. The acid species in Figure 7 are denoted by the number of carbon atoms to the number of double bonds (e.g., oleic acid $[C_{17}H_{33}COO]^-$ = 18:1 at m/z 281). Ions from the C_{16} and C_{18} acid moieties are observed. Figure 7b shows the OH^- CI/FAB mass spectrum of pure olive oil. The ion abundances are almost 300 times greater than those in Figure 7a. Therefore, the CI/FAB method allows a greater sensitivity for the analysis. Mixed proton-bound dimers of the carboxylate anions are observed at high mass, that is, $[(16:0)^-\cdots H^+\cdots(18:1)^-]$ (m/z 537), $[(18:1)^-\cdots H^+\cdots(18:2)^-]$ (m/z 561), $[(18:1)^-\cdots H^+\cdots(18:1)^-]$ (m/z 563), and $[(18:1)^-\cdots H^+\cdots(18:0)^-]$ (m/z 565).

We have found that the relative abundances of the fatty acid species observed by this mass spectrometric method agrees very well with the results obtained by the gas chromatography of the fatty acid methyl esters.[27] The FAB mass spectrometric analysis of lipids enables a rapid and direct screening of the fatty acid content. We have applied this method to the direct analysis of fatty acids in the lipid content of algal cells.[27]

Conclusions

The combination of chemical ionization and fast-atom bombardment has resulted in 2–3 orders of magnitude enhancements of molecular parent ions through various ion/molecule reactions. These reactions have been shown to include collisional stabilization, charge-exchange, proton-transfer, and association reactions. The relative enhancement of the secondary molecular ions by collisional stabilization was found to be dependent on the relative collisional stabilization efficiency of the bath gas. In other words, fragment ions produced by unimolecular dissociations of the molecular species are decreased in abundance due to the collisional stabilization of their sputtered precursors by various bath gases. Charge exchange, chemical ionization, and adduct formation also can lead to enhancement of the molecular parent ion abundance by the postdesorption ionization of sputtered neutral species in the chemical ionization plasma. Several of these ion/molecule effects may be combined in an optimal experiment to provide a selective, sensitive analytical technique.

Another advantage of this method is increased sample lifetime. For example, the abundance of the molecular ion of chlorophyll A has been observed for an order of magnitude in time longer in the CI/FAB source than in the conventional FAB source. Experiment indicates that this is due to the attenuation of the fast-atom beam by its small aperture in the ion source. This attenuation results in a lower rate of radiation damage to the reservoir of sample molecules (sample and matrix) because the fast-atom beam density is decreased an order of magnitude.

As of this time, the use of conventional liquid matrices has been prohibitive because of their high proton affinities (215–225 kcal/mol) relative to the sample. This results in dramatic increases in the ion abundances of the matrix-type ions. In other words, the chemical noise is increased tremendously when this method is used with a conventional liquid matrix. It may be possible to use novel matrixes and matrix/reactant gas combinations that can enhance selectively the abundance of a sample from the liquid substrate. Thus far, neat liquid samples have provided the most versatility.

Studies have been extended in our laboratory to encompass the technique of chemical ionization/molecular secondary ion mass spectrometry (CI/SIMS).[30] In the molecular SIMS technique, organic species are desorbed from a solid substrate by using a diffuse, low-fluence primary beam.[5,8] Similarly, the abundant secondary neutrals can be ionized by ion/molecule reactions as in the CI/FAB technique. The advantage of the CI/SIMS method is that a liquid matrix is not required, and because only a molecular overlayer is probed, the chemical noise is decreased tremendously. More recently, we have used this CI/SIMS concept to study the reactions of sputtered metal cluster ions with organic reactants.[31] The metal-organic cluster ion reaction products were

(26) Smit, A. L. C.; Field, F. H. *J. Am. Chem. Soc.* **1977**, *99*, 6471–6483.
(27) Ross, M. M.; Neihof, R. A.; Campana, J. E., submitted for publication.
(28) Hendricks, H. A.; Bruins, A. P., *J. Chromatogr.* **1980**, *190*, 321–330.
(29) Tomer, K. B.; Crow, F. W.; Gross, M. L. *J. Am. Chem. Soc.* **1983**, *105*, 5487–5488.
(30) Ross, M. M.; Freas, R. B.; Campana, J. E., unpublished work.
(31) Freas, R. B.; Campana, J. E. *J. Am. Chem. Soc.*, following paper in this issue.

characterized by using tandem mass spectrometric techniques, and the information obtained was indicative of C–C and C–H metal insertion reactions. Still other possibilities exist to study the ion chemistry of intractable species by use of the technique described here.

Acknowledgment. This work was supported by the Office of Naval Research.

Appendix

Collisional Stabilization Efficiencies. The collisional stabilization efficiency of an atomic or molecular species, M, is a measure of its ability to remove excess internal energy from an excited species upon collision, for example

$$AB^{+*} + M \xrightarrow{k_M} AB^+ + M + \text{energy} \quad (1)$$

By simple approximation, the collisional stabilization rate constants k_M or the overall three-body attachment rate constants K_M (as will be shown later) for a series of bath gases can provide some relative measure of the collisional stabilization efficiencies. Unimolecular reaction theory gives the approximation $K_M[M] = \lambda Zp$ where λ is the collisional stabilization efficiency, Z is the collision number, and p is the pressure.[32] The value of Z is approximately the same for all collision partners.[33] This is because the collision number contains a number of constant terms and a factor $(\sigma^2/\mu^{1/2})$, where σ is the collision diameter and μ is the reduced mass. This factor varies by a factor of 2–3 for most collision pairs. Therefore, at constant [M] and p,

$$\lambda = CK_M \text{ or } \lambda \propto K_M \quad (2)$$

More rigorous treatments to this approximation have been reviewed.[21]

We calculate the relative collisional stabilization efficiencies for He, Ar, Xe, CH_4, CO, CO_2, and i-C_4H_{10} using one of the more rigorous methods.[34] We have used the tabulated overall three-body attachment rate constants, K_M,[34,35] for the reaction

$$O_2 + e \underset{k_d}{\overset{k_a}{\rightleftharpoons}} O_2^{-*} + M \xrightarrow{k_M} O_2^- + M \quad (3)$$

(The reaction $O_2^{-*} + O_2 \xrightarrow{k} O_2^- + O_2$ (not shown) is negligible at high pressures of M.) The overall three-body attachment rate constant is given by

$$K_M = (k_a/k_d)k_M \quad (4)$$

The electron attachment and detachment rates will be independent of the bath gas M so that K_M can be considered to depend directly on the collisional stabilization rate constant k_M. The collisional stabilization reaction can be envisioned to occur in two steps, (i) the collision, with rate constant k_c, and (ii) the transfer of excess energy from AB^{+*} (reaction 1) or O_2^{-*} (reaction 3) to M with probability P_M. Therefore, k_M can be expressed

$$k_M = k_c P_M \quad (5)$$

The collision rate can be calculated[36] from

$$k_c = 2\pi e(\alpha/\mu)^{1/2}$$

where α is the polarizability of M. Substituting eq 5 into eq 4 gives

$$K_M/k_c = (k_a/k_d)P_M \propto P_M \quad (6)$$

The K_M values taken from ref 34 and 35 (divided by 10^{-30} cm^6 molecule^{-2} s^{-1}) are He (0.33), Ar (0.05), Xe (0.085), CO (1.31), CO_2 (3.00), CH_4 (0.34), n-C_4H_{10} (5.00), and neo-C_5H_{12} (7.90). These values were applied to eq 6 to determine the relative P_M values. The relative P_M values were normalized to a value of 1.00 for He as is customary.[21] Because there were not K_M values tabulated for the O_2–(i-C_4H_{10}) system, we assumed that the K_M for isobutane would be about the same as the five-membered branched hydrocarbon, neopentane, whose value was used to obtain the isobutane relative collisional stabilization efficiency plotted in Figure 2. Approximating the $K_{isobutane}$ to $K_{n\text{-butane}}$ also gave a good result. Furthermore, using the simple approximation, given in eq 2, also gives results comparable to those illustrated in Figure 2.

We suggest that the O_2–M system might be an ideal system to obtain relative collisional stabilization efficiencies. In particular, this simple reaction (eq 3) depends strongly on the nature of M, it has been studied in detail,[35] K_M values exist for a variety of bath gases, and the simple approximation for collisional stabilization efficiency (eq 2) may be used. As usual, caution must be used even when the K_M data are used qualitatively as illustrated for xenon (vide infra).

(32) Robinson, P. J.; Holbrook, K. A. "Unimolecular Reactions"; Wiley Interscience: New York, 1972, p 104.
(33) Forst, W. "Theory of Unimolecular Reactions"; Academic Press: New York, 1973, p 184.
(34) Shimamori, H.; Hatano, Y.; *Chem. Phys.* **1977**, *21*, 187–201.
(35) Hatano, Y.; Shimamori, H. "Electron and Ion Swarms"; Christophorou, L. G., Ed.; Pergamon Press: New York, 1981, pp 106–107.
(36) Gioumousis, G.; Stevenson, D. P. *J. Chem. Phys.* **1958**, *29*, 294–299.